Journal of
PERIODONTAL RESEARCH

J Periodont Res 2013; 48: 663–670

JOURNAL OF PERIODONTAL RESEARCH
doi:10.1111/jre.12062

Contour analysis of an implant–soft tissue interface

W. L. Chai[1], K. Moharamzadeh[2], R. van Noort[2], L. Emanuelsson[3], A. Palmquist[3], I. M. Brook[4]

[1]Department of General Dental Practice and Oral & Maxillofacial Imaging, Faculty of Dentistry, University of Malaya, Kuala Lumpur, Malaysia, [2]Academic Unit of Restorative Dentistry, School of Clinical Dentistry, University of Sheffield, Sheffield, UK, [3]Department of Biomaterials, Sahlgrenska Academy, University of Gothenburg, Gothenburg, Sweden and [4]Academic Unit of Oral & Maxillofacial Surgery and Medicine, School of Clinical Dentistry, University of Sheffield, Sheffield, UK

Chai WL, Moharamzadeh K, van Noort R, Emanuelsson L, Palmquist A, Brook IM. Contour analysis of an implant–soft tissue interface. J Periodont Res 2013; 48: 663–670. © 2013 John Wiley & Sons A/S. Published by John Wiley & Sons Ltd

Background and Objective: Studies of peri-implant soft tissue on *in vivo* models are commonly based on histological sections prepared using undecalcified or 'fracture' techniques. These techniques require the cutting or removal of implant during the specimen preparation process. The aim of this study is to explore a new impression technique that does not require any cutting or removal of implant for contour analysis of soft tissue around four types of titanium (Ti) surface roughness using an *in vitro* three-dimensional oral mucosal model (3D OMM).

Methods: The 3D OMM was constructed by co-culturing a keratinocyte cell line TR146 and human oral fibroblasts on to an acellular dermis scaffold. On the fourth day, a Ti disk was placed into the model. Four types of Ti surface topographies, i.e. polished, machined, sandblasted and anodized were tested. After 10 d of culture, the specimens were processed based on undecalcified (ground sectioning), electropolishing and impression techniques for contour analysis of the implant–soft tissue interface.

Results: Under light microscopic examination of the ground and electropolishing sections, it was found that the cell line-based oral mucosa formed a peri-implant-like epithelium attachment on to all four types of Ti surfaces. In contour analysis, the most common contour observed between the cell line-based oral mucosa and Ti surface was at an angle ranging between 45° and 90°.

Conclusion: The *in vitro* cell line-based 3D OMM formed a peri-implant-like epithelium at the implant–soft tissue interface. The contour of the implant–soft tissue interface for the four types of Ti surface was not significantly different.

Dr. Wen Lin Chai, BDS, MDSc, PhD, FDSRCS, Department of General Dental Practice and Oral & Maxillofacial Imaging, Faculty of Dentistry, University of Malaya, Kuala Lumpur 50603, Malaysia
Tel: +603-79674895
Fax: +603-79674575
e-mail: chaiwl@um.edu.my

Key words: dental implant; epithelium; fibroblast; *in vitro* model; tissue engineering

Accepted for publication January 15, 2013

The peri-implant tissue responses especially in relation to the osseointegration of various dental implant surfaces have been widely reported. As important as the hard tissue response, the soft tissue around the implant plays an important role in determining the long-term success of dental implant treatment (1–3). It forms a biological seal around the implant to protect the underlying tissue from the invasion of microorganism.

The soft tissue component of implants consists of peri-implant epithelium and fiber connective tissue at the coronal and apical part of the implant, respectively (1,3–5). Studies have shown that the soft tissue response was influenced by various factors such as implant surface topography (6), abutment materials (7,8), implant systems (9,10) and surgical techniques (11,12). These types of studies were usually carried out on animal models, in which the peri-implant mucosa, or its biologic width has been widely reported. The sample preparation for the histomorphometric analysis of the implant–tissue interface is mainly based on two methods (13), i.e. undecalcified/ground sectioning techniques (12) or 'fracture' techniques (14). In undecalcified/ground sectioning technique, the whole specimens containing the implant metal were embedded, cut

and grounded into thin ground sections. Hence, the implant metal remained intact in the final ground sections, which provides an intact implant–tissue relationship at the interface for analysis. However, it is a technical demanding procedure as the specimens contain different types of 'materials', i.e. the hard metal implant (titanium, Ti) and soft tissue. The soft tissues would be grounded more than the metal surface, resulting in an uneven histological section. In contrast, the 'fracture' technique separates the implant (Ti) from the specimen before being processed for histological sections. An example of this technique is by dissolving the bulk of the Ti implant using an electropolishing technique. However, the disadvantage of implant removal is that it leaves a 'space' in histological sections. Hence, evaluation of the direct relationship of the tissue to the implant surface at the interface may be compromised. Thus, both techniques have their limitations. A more detailed discussion of the advantages and disadvantages of the sample preparation techniques for the implant–soft tissue interface analysis have been reported (13).

In this paper, we would like to report a simple technique, which is without any involvement of cutting or separation of the implant, for the implant–soft tissue interface investigation. In our previous study (15), an *in vitro* primary cell-based oral mucosa model has been developed and showed a peri-implant-like epithelium (PILE) attached to the Ti surfaces as seen in animal models. In this study, a cell line-based three-dimensional oral mucosal model (3D OMM) was constructed. The aim of this study was to explore a new impression technique to analyze the contour between the cell line-based oral mucosa and Ti surfaces of four different types of Ti surface topographies. Three sample preparation techniques for the implant–soft tissue interface analysis were reported, including ground sectioning, electropolishing and impression techniques.

Material and methods

Construction of a cell line-based three-dimensional oral mucosal model

In this study, a cell line-based 3D OMM was constructed using modification of a previous oral mucosal model (15). Ethical approval was obtained from the North Sheffield Research Ethics Committee. An acellular human cadaveric dermis (Alloderm, LifeCell, Branchburg, NJ, USA) of 0.9 mm thickness was cut into a 12 mm diameter disk before rehydrated in culture medium for about 15 min. The rehydrated dermis was then placed into 12 mm diameter inserts, which have 0.4 μm pore size and 1×10^8 pore density/cm^2 (Costar 12 mm Snapwell Insert, Corning Life Sciences, Corning, NY, USA). An epithelial cell line TR146 (a gift from Cancer Research UK) and human oral fibroblasts (passages 2–5) from frozen stocks were de-frozen and cultured in Dulbecco's modified Eagle's medium containing 50 U/mL penicillin, 50 U/mL streptomycin and 625 ng/mL fungizone (the agents mentioned above were purchased from Sigma-Aldrich, Dorset, UK), supplemented with 10% fetal calf serum (Biowest, East Sussex, UK). When the cells reached confluence, a 150 μL of cell suspension with a mixture of TR146 and human oral fibroblasts at a density of 0.5×10^6 each was prepared and inoculated on to the basement membrane side of the acellular dermis. Each well was then filled with 5.5 mL of culture medium in a six-well plate. These models were incubated in an incubator at 37°C in an atmosphere of 95% air/5% carbon dioxide (Galaxy R®, Scientific Laboratory Supplies Ltd. East Riding of Yorkshire, UK) for 3 d. On the fourth day of culture, a 4 mm diameter hole was prepared using a sterile disposable tissue biopsy punch (Stiefel Laboratories, Bucks, UK). A Ti disk (5 mm diameter × 2.5 mm height) was then placed into the punched hole. Four types of Ti surfaces were tested, in which the polished, machined (turned) and sandblasted surfaces were prepared from a commercially pure grade-4 Ti rod (grant 2008-757, Nobel Biocare) using in-house equipment, and the anodized disks (TiUnite®) were prepared by Nobel Biocare (Gothenburg, Sweden). The 3D OMM was further cultured in submerged position in the medium (as above), and gradually reduced to near air–liquid interface over a period of 6 d.

Characterization of the three-dimensional oral mucosa

The 4 mm punched oral mucosal equivalent (OME) obtained during the 4 mm hole preparation was cultured parallel with the 3D OMM. At the end of the culture, the punched tissue was characterized using immunohistochemistry staining based on the avidin–biotin complex method (15). A human gingival buccal mucosa biopsy was used as the control. Briefly, the formalin-fixed, wax-embedded sections were dewaxed in xylene and rehydrated through a graded alcohol series. The sections were then treated with 0.3% hydrogen peroxide in methanol to inhibit endogenous peroxidase. The antigens were then retrieved by incubating in 0.1% trypsin at 37°C for 20 min. Mouse monoclonal primary antibodies (Vector Labs, Burlingame, CA, USA) of CK10 and CK13 at a concentration of 1 : 50 and 1 : 200 respectively were used to stain the keratinocyte antigens in the epithelium. Following that, the sections were treated with biotinylated antimouse secondary antibodies (Vector Labs). The reactions were visualized by staining with 0.05% diaminobenzidine and then counterstained with hematoxylin for light microscopy (LM) examination.

Interface examination

Three sample preparation techniques were employed for interface examination, i.e. ground sectioning (undecalcified), electropolishing and impression techniques.

Ground sectioning technique— At the end of the 10 d culture period, the 3D

OMM was fixed with 2.5% glutaraldehyde in 0.05 M sodium cacodylate buffer at pH 7.15 for 2–3 d, and post-fixed with 1% O_SO_4 for 2 h. It was then dehydrated in a series of ascending concentrations of ethanol, i.e. 50%, 70%, 90%, 95% and 100% and 1,2-propylene oxide for 60 min each, in which two changes of solution for each concentration were carried out. The specimens were then pre-infiltrated in a mixture of 1,2-propylene oxide/epoxy resin (1 : 1) for 2 h followed by infiltration in pure epoxy resin (Agar Scientific Ltd., Stansted, Essex, UK) overnight. Following that, the specimens were embedded in new epoxy resin and polymerized at 40°C for 15 h and finally at 60°C for 48 h. The embedded specimens were then cut in half using a diamond band saw (0.1 mm D32) on a cutting machine (Exakt 300, Exakt Apparatebau, Norderstedt, Germany). One-half of the block was prepared using the ground sectioning technique, while the other half was prepared using the electropolishing technique.

For ground sectioning, the half block was re-embedded in acrylic resin (LR White, London Resin Company, London, UK) with the cut surface exposed for polishing. Under constant pressure, the cut surface of the re-embedded block was polished on a grinding machine (Exakt 400CS, Exakt Apparatebau) using waterproof silicon carbide papers of grit P1200 (Struers, Gothenburg, Sweden). After achieving a satisfactory polished surface, the cut surface was glued on to a plastic slide with Technovit 7210 VLC resin (Heraeus Kulzer GmbH, Wehrhelm, Germany) and polymerized with a light source (Exakt-precision adhesive system, Kulzer, Norderstedt, Germany). Subsequently, the glued block was cut into a 100–150 μm thick section using a diamond band saw on a cutting machine (Exakt 300, Exakt Apparatebau). The thickness of the thin section was further reduced to 25–30 μm by grinding and polishing on silicon carbide papers under a constant pressure on the grinding machine. Lastly, the ground sections were stained in 10% hydrogen peroxide (H_2O_2) for 10 min followed by Richardson solution (equal parts of 1% azure II and 1% methylene blue in 1% borax) (16) for 30 min before LM examination.

Electropolishing technique— The other half of the epoxy resin block was processed with the electropolishing technique (15). Briefly, the bulk of the Ti metal was dissolved in an electrolytic solution, consisting of 5% perchloric acid, 35% n-butanol and 60% methanol at −30°C. In the setup, the specimens served as cathode, while a platinum ring around the specimens served as the anode. The electropolishing process was performed at 200 mA/cm^2 and 24V for about 4–5 h. The dissolved blocks were then cut into semithin sections (1–1.5 μm thick) using glass knives on a microtome (Ultracut Reichert-Jung, ISS Group Services, Manchester, UK). Following that, the semithin sections were stained with toluidine blue and then examined under LM.

Impression technique— For contour analysis of the interface, the 3D OMM was duplicated into a silicone model using two different colored light-bodied silicone impression materials (Aquasil Ultra LV, Smart Wetting® Impression Material, Dentsply Caulk International Inc., Milford, DE, USA). Briefly, at the end of the 10 d culture period, an orange-colored light-bodied silicone impression material was carefully injected onto each 3D OMM to record the contour of the interface of the cell line OME and the Ti surface. After setting, the orange silicone was separated from the models. Following that, a blue light-bodied silicone was injected into the set orange impression materials (Fig. 1A). Subsequently, the duplicated silicone models were cut with a scalpel blade at north to south, east to west, northeast to southwest and northwest to southeast directions (Fig. 1A). Hence, eight sites for each sample could be examined under a stereomicroscope (Discovery V8, Carl Zeiss, Jena, Germany). The angle between the OME and the Ti disk at the interface (see inset in Fig. 1A) was categorized into the following three scores: (i) score 1 : $< 45°$ (Fig. 1B); (ii) score 2 : $45° \leq \times \leq 90°$ (Fig. 1C); and (iii) score 3 : $> 90°$ (Fig. 1D).

A total of ten 3D OMMs ($n = 10$) in which two samples for each Ti surface (polished, machined, sand-blasted and anodized surfaces) and a negative control group (i.e. an acellular dermis without any cells) were prepared. The percentage of the frequency of each score in each group was calculated. The comparison among the four Ti surfaces and negative control group was analyzed using a non-parametric Kruskal–Wallis test.

Results

Characterization of the oral mucosal equivalent

The cell line-based OME (Fig. 2A) has shown some mimicking features such as a well formed stratified squamous epithelium as seen in the normal oral mucosa (Fig. 2D). In the immunohistochemistry analysis, the cell line OME showed a strong expression of CK10 (a keratinized epithelial marker; Fig. 2B), but a weak expression of the CK13 (a non-keratinized epithelial marker; Fig. 2C) at the suprabasal layer. Figure 2E and 2F represent the positive control for the CK10 and CK13 in normal oral mucosa respectively. This observation suggests that the cell line OME has a closer feature to a keratinized oral epithelium.

Interface examination— Figure 3 represents the results of the LM examination of the interface for the four types of Ti surfaces in ground (Fig. 3A–G) and semithin sections (Fig. 3H–O). During the ground section preparation for the machined group, one side of the tissue was dislodged from the slide, while the Ti disk on the other side was detached from the section during the grinding procedure, leaving a Ti 'space' at the interface area (Fig. 3C). While in the semithin sections, the bulk of the Ti had been removed during the electropolishing technique leaving a 'space' at the interface. However, a thin Ti oxide layer still remained

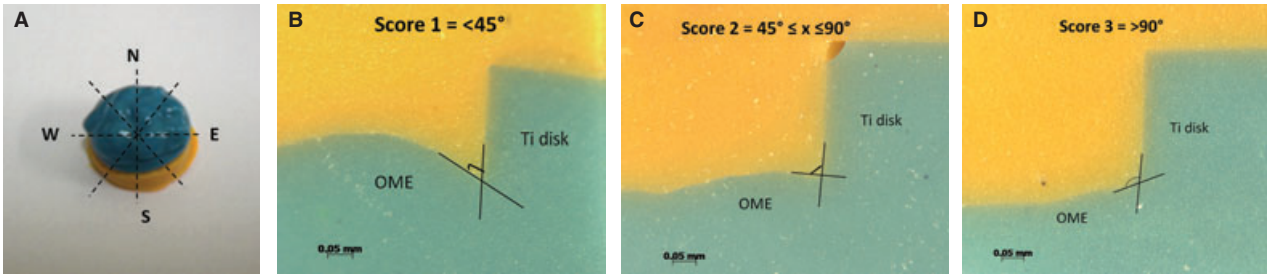

Fig. 1. (A) An impression technique was used to duplicate the three-dimensional oral mucosal model to a silicone model. The dashed lines indicate the slices made with a scalpel on the silicone model to expose the contour of the interface. The angle between the oral mucosa (OME) and the titanium (Ti) disk (arrows in the insert) were classified into three scores, i.e.: (B) score 1, < 45; (C) score 2, 45° ≤ × ≤ 90; and (D) score 3, > 90°. Scale bar = 50 μm.

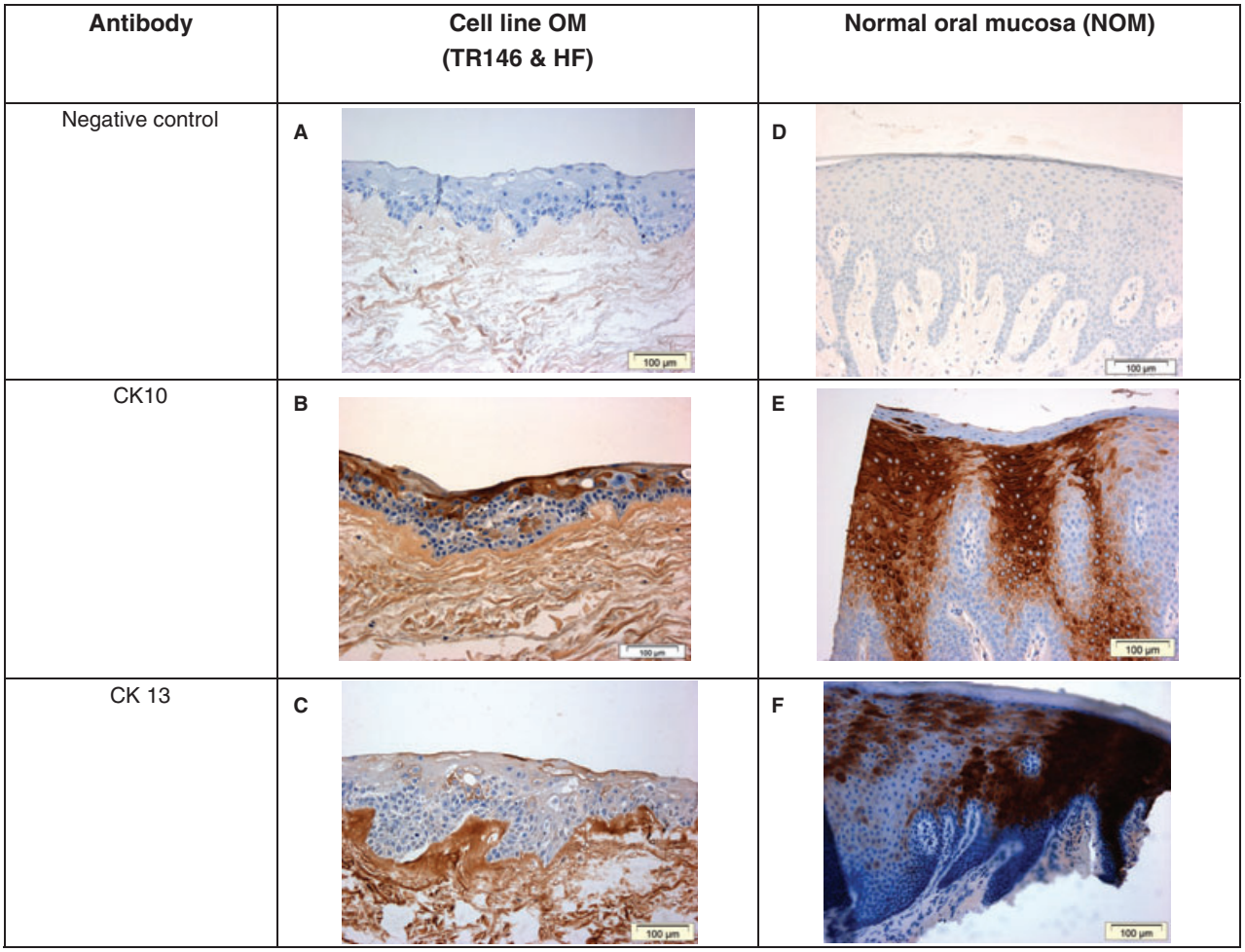

Fig. 2. Immunohistochemistry staining of the oral mucosa. (A,D) Negative control for cell line and normal oral mucosa respectively. It was noticed that the cell line oral mucosal model shows strong expression of CK10 at the suprabasal layer (B), but weak expression of CK13 (C). Both epithelial markers were well detected at the suprabasal epithelial layer of the normal oral mucosa (E,F). Scale bar = 100 μm.

intact at the interface in sandblasted (Fig. 3L,3M) and anodized groups (Fig. 3N,3O) even though the bulk of the Ti metal had been removed. This feature provides an advantage for an intact interface examination. It showed that both the sandblasted (Fig. 3L,3M) and anodized (Fig. 3N,3O) surfaces appeared to be more irregular than the polished (Fig. 3H,3I) and machined surfaces (Fig. 3J,3K). In addition, the semithin sections (Fig. 3H–O) showed more detailed structures compared to the corresponded ground sections (Fig. 3A–G).

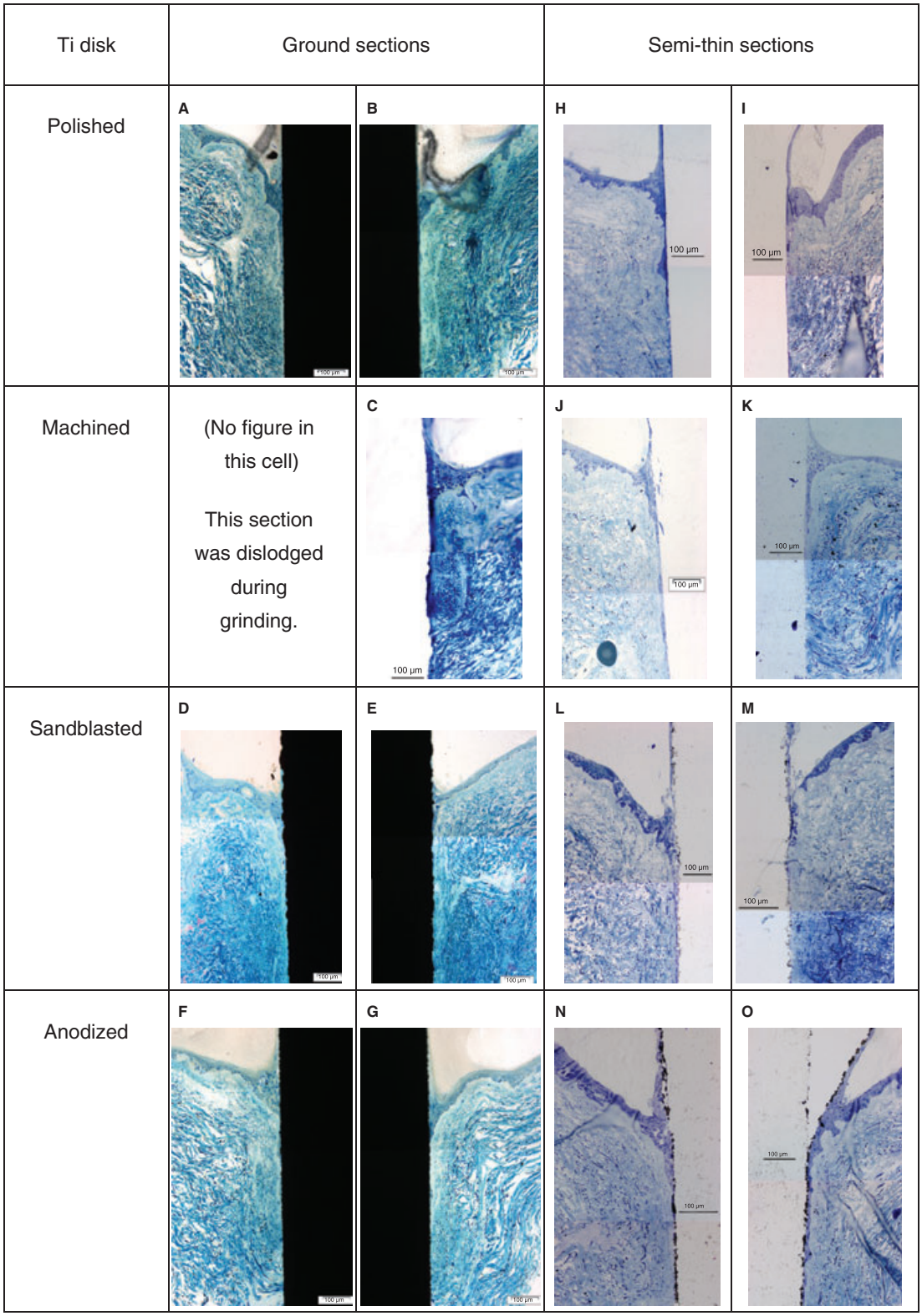

Fig. 3. A comparison of ground and semithin sections of the 3D OMMs for polished, machined, sandblasted and anodized groups. (A,B) Ground sections of the left and right sides of the interface in the polished group. The titanium (Ti) disk of the machine group was dislodged in the ground section, left a Ti space (C). (D–G) Ground sections of both side of the interface in the sandblasted and anodized groups respectively. (H–O) Semithin sections on both sides of the interface in the polished, machined, sandblasted and anodized groups respectively. In all sections, it was noted that peri-implant-like epithelium attached to the Ti surfaces at the interface. Scale bar = 100 µm.

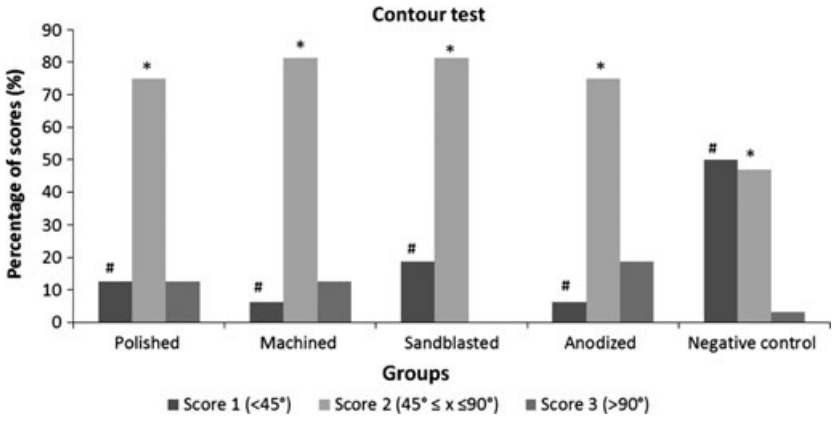

Fig. 4. A comparison of the percentage of scores of four titanium groups and a negative control group based on the silicone model in contour analysis. #A significant higher percentage of score 1 in negative control group than the titanium groups. *A significant higher percentage of score 2 observed in titanium groups compared to negative control group.

On examination of the OME structure at the interface area, it was observed that the OME formed PILE next to the Ti surfaces. A 'non-pocket' type of epithelial attachment, which refers to the absence of gap between the epithelium and the Ti surface, was noticed in all sections (Fig. 3). Interestingly, it was also noticed that PILE appeared to migrate upward on to the Ti surfaces forming a 'slope' contour at the interface (see Fig. 3C–L,3N,3O).

The contour at the interface was evaluated in the impression technique. From the silicone models, the frequency of each score of the interface for the four Ti groups and a negative control was obtained. The frequency of each score is presented as percentage of scores for each group as shown in Fig. 4.

It was found that score 2, i.e. an OME attached to the Ti disk at an angle ranged from 45° to 90°, was the most frequently observed contour ($p < 0.05$). This contour was observed in 75%, 81%, 81% and 75% in polished, machines, sandblasted and anodized groups, respectively. The percentage of score 2 was not significantly different within the Ti groups but was significantly higher than the negative control group (47%).

In contrast, compared with the Ti groups, the negative control group had a significant highest percentage of score 1, which has an acute angle of < 45° ($p < 0.05$).

Score 3, which has an angle of soft tissue attachment at an angle of more than 90°, is the least observed contour in all the test groups. No statistical difference was observed in the test groups.

Contour analysis suggests that regardless of the different Ti surface topographies (polished, machined, sandblasted or anodized), the OME attached to the Ti surfaces in a rather similar contour, i.e. usually at an angle ranging from 45° to 90°.

Discussion

The OME constructed by co-culturing keratinocyte cell line TR146 and human oral fibroblasts on the acellular dermis has shown features mimicking normal oral mucosa (Fig. 2D). There were three to four layers of epithelial cells formed on the epithelium of the OME (Fig. 2A–C). These features were similar to that seen in our previous study using primary cells for the construction of OME (15). Both primary and cell line OMEs revealed well formed stratified squamous epithelium. Hence, both the primary and cell line 3D OMMs are more representative of an *in vivo* model compared to a 2D monolayer cell culture model.

However, there are several disadvantages when using primary cells for OME construction, such as a limited source of biopsies, variation of the donors and short lifetime of the cells (17). As an alternative in this study, epithelial cell line TR146 (18) was used for the construction of an *in vitro* model. The advantage of using cell line OMEs is that a larger number of samples could be produced in a more consistent and controlled manner compared to the use of primary cells. Several investigators have used cell line OMEs for various *in vitro* studies (17,19–21). Figure 3 suggested that cell line-based OME also formed PILE at the interface as seen in our previous primary oral mucosal model (15), in which it had been used in the implant–soft tissue interface investigation.

In this study, the interface between the OME and the Ti surfaces were examined using three different sample preparation techniques, i.e. ground sectioning, electropolishing and impression techniques. The first two techniques provide descriptive features of the interface, while the latter technique allows a quantitative analysis of the contour by comparison of the angle between the OME and Ti at the interface region.

In the ground sectioning technique, one of the merits of this technique is that it preserves a direct relationship between soft tissue and the Ti surface at the interface (Fig. 3A–G). However, the disadvantage of the ground sectioning technique is that it is a demanding procedure (13). The specimens containing both metal and soft tissue pose difficulty in obtaining a flat surface during the grinding procedure, as the soft tissue was usually ground faster than the metal implant, and resulted occasionally in loss of the section during preparation as seen in one of our samples (see Fig. 3C). Thus, one has to be aware that some specimens will be lost during the ground sectioning preparation technique.

While in the electropolishing technique, the bulk of Ti was removed leaving a Ti space at the interface area, it may result in difficulty in determining the direct relationship of PILE to the Ti surface at the interface (Fig. 3H–O). However, it was noticed that in both the sandblasted (Fig. 3L,3M) and anodized (Fig. 3N,3O) semithin

sections, a very thin residual Ti oxide layer remained intact at the interface. Hence, this allowed evaluation of the relationship of PILE to the Ti surfaces in these two groups.

In this study, the same specimen was embedded before cutting in half, in which one half was prepared for ground sections and the other half for semithin section preparation. Hence, a comparison of a histological section that contained Ti (ground sections, Fig. 3A–G), and without Ti (semithin sections, Fig. 3H–O) of the same specimen could be made under LM examination. Another interesting finding in this study is that semithin sections revealed more detailed structures compared to the corresponding ground sections. This could be attributed to the fact that after removal of Ti bulk, a very thin semithin section, i.e. 1.5 μm could be achieved compared to a ground section (30 μm). Nevertheless, under LM examination, both ground and semithin sections showed that the OME epithelium proliferated and differentiated into PILE, as similar to the peri-implant epithelium structure seen in animal models. The PILE attached to the Ti surfaces regardless of the different types of surface roughness. In other words, the surface topography does not have a significant influence on the soft tissue attachment. This finding is consistent with an animal study, which had reported that there is no significant histomorphometric analysis between the turned (smooth) and acid-etched (rough) implants (3).

Lastly, in this study, a new method was explored using an impression technique for contour analysis of the Ti–OME interface. To our knowledge, this is the first time that a contour between the soft tissue and Ti surface at the interface is being evaluated using an *in vitro* 3D OMM. A low viscosity of silicon impression material was used, as it is able to flow into the gap at the interface and records the fine details of the contour adjacent to the Ti surface. The 3D OMM was then duplicated into silicone polymer models. With a very simple way of cutting through silicone polymer models by scalpel, the contour of the OME at the interface can be assessed. Besides the easy preparation technique, the silicone polymer model provides eight sites of interface per sample for analysis possibly minimizing the loss of sections as seen with other techniques such as ground sectioning or electropolishing preparations.

In contour analysis, the score 1 (< 45°) was commonly found in the negative control group, which does not contain any cell attachment to the Ti surfaces, thus forming an acute angle at the interface. In contrast, the score 2, with an angle ranges from 45° to 90° between the OME and Ti surface, was the most commonly observed contour in the Ti groups. This may suggest that the cells from the OME attached to the Ti surfaces forming a seal around them. However, these cells may not be able to migrate/'climb' upward to the Ti surface to form an angle of > 90° as seen in score 3.

In our previous study (15), we have reported two types of soft tissue attachments, i.e. 'pocket' and 'non-pocket' on the Ti surfaces in 3D OMM. Clinically, the 'non-pocket' type of attachment could be related to a more favorable attachment than the 'pocket' type, as the latter has a higher risk of plaque retention, which may result in peri-implantitis. In this study, only a 'non-pocket' type of soft tissue attachment was present in the cell line-based 3D OMM. However, when compared to the result of contour analysis in silicone models, where more areas of interface could be examined, it revealed that both 'non-pocket' (corresponding to scores 2 and 3) and 'pocket' (score 1) type of epithelial attachments were actually present in the cell line-based models.

In summary, the cell line-based 3D OME, which has shown formation of PILE attachment to the Ti surfaces, allowed quantitative investigation of the soft tissue response to implant surfaces. However, this *in vitro* model still lacks some other connective tissue components of the peri-implant tissue as present in the animal and human models, which could not be verified in this cell line-based 3D OMM. This could be a major drawback of this model. The new method described in this study for contour analysis of the soft tissue–implant interface provides useful information on the types of favorable implant surfaces for soft tissue attachment.

Conclusion

The cell line-based 3D OMM formed PILE on to the Ti surface. Contour analysis of the silicone model provided useful quantitative information on the contour of the OME attachment on the Ti surfaces. The contour of the soft tissue attachment on four types of Ti surface topographies tested in this study was not significantly different.

Acknowledgements

The first author would like to convey her gratefulness towards the Government of Malaysia of the scholarship offered for her PhD study in the University of Sheffield and being granted a research grant (UM.C/625/1/HIR/MOHE/DENT/05) for furthering this research at the University of Malaya. The authors would like to thank Prof. Peter Thomsen for his advices and Birgitta Norlindh for her technical support (both are from BIOMATCELL VINN Excellence Center of Biomaterials and Cell Therapy, Gothenburg, Sweden). We also like to thank the Cancer Research Center, UK for providing the keratinocyte cell line TR146, and Nobel Biocare for supplying the TiUnite Ti disks and commercial pure Ti (grant no. 2009-757).

References

1. Kawahara H, Kawahara D, Hashimoto K, Takashima Y, Ong JL. Morphologic studies on the biologic seal of titanium dental implants. Report I. In vitro study on the epithelialization mechanism around the dental implant. *Int J Oral Maxillofac Implants* 1998;**13**:457–464.
2. Carmichael R, Apse P, Zarb G, Mcculloch C. Biological, microbiological and clinical aspects of the peri-implant mucosa. In: Albrektsson T, Zarb G, eds. *The Branemark Osseointergrated Implant*. Chicago: Quintessence, 1989:39–78.

3. Abrahamsson I, Zitzmann NU, Berglundh T, Linder E, Wennerberg A, Lindhe J. The mucosal attachment to titanium implants with different surface characteristics: an experimental study in dogs. *J Clin Periodontol* 2002;**29**:448–455.
4. Berglundh T, Abrahamsson I, Welander M, Lang NP, Lindhe J. Morphogenesis of the peri-implant mucosa: an experimental study in dogs. *Clin Oral Implants Res* 2007;**18**:1–8.
5. Hermann J, Buser D, Schenk R, Higginbottom F, Cochran D. Biologic width around titanium implants. A physiologically formed and stable dimension over time. *Clin Oral Implants Res* 2000;**11**:1–11.
6. Abrahamsson I, Zitzmann NU, Berglundh T, Wennerberg A, Lindhe J. Bone and soft tissue integration to titanium implants with different surface topography: an experimental study in the dog. *Int J Oral Maxillofac Implants* 2001;**16**:323–332.
7. Abrahamsson I, Berglundh T, Glantz PO, Lindhe J. The mucosal attachment at different abutments. An experimental study in dogs. *J Clin Periodontol* 1998;**25**:721–727.
8. Buser D, Weber HP, Donath K, Fiorellini JP, Paquette DW, Williams RC. Soft tissue reactions to non-submerged unloaded titanium implants in beagle dogs. *J Periodontol* 1992;**63**:225–235.
9. Abrahamsson I, Berglundh T, Lindhe J. Soft tissue response to plaque formation at different implant systems. A comparative study in the dog. *Clin Oral Implants Res* 1998;**9**:73–79.
10. Arvidson K, Fartash B, Hilliges M, Kondell PA. Histological characteristics of peri-implant mucosa around branemark and single-crystal sapphire implants. *Clin Oral Implants Res* 1996;**7**:1–10.
11. Hermann JS, Buser D, Schenk RK, Schoolfield JD, Cochran DL. Biologic width around one- and two-piece titanium implants. *Clin Oral Implants Res* 2001;**12**:559–571.
12. Weber HP, Buser D, Donath K *et al*. Comparison of healed tissues adjacent to submerged and non-submerged unloaded titanium dental implants. A histometric study in beagle dogs. *Clin Oral Implants Res* 1996;**7**:11–19.
13. Chai WL, Moharamzadeh K, Brook IM, van Noort R. A review of histomorphometric analysis techniques for assessing implant-soft tissue interface. *Biotech Histochem* 2011;**86**:242–254.
14. Rosengren A, Johansson BR, Danielsen N, Thomsen P, Ericson LE. Immunohistochemical studies on the distribution of albumin, fibrinogen, fibronectin, IgG and collagen around PTFE and titanium implants. *Biomaterials* 1996;**17**:1779–1786.
15. Chai WL, Moharamzadeh K, Brook IM, Emanuelsson L, Palmquist A, van Noort R. Development of a novel model for the investigation of implant-soft tissue interface. *J Periodontol* 2010;**81**:1187–1195.
16. Richardson KC, Jarett L, Finke EH. Embedding in epoxy resins for ultrathin sectioning in electron microscopy. *Stain Technol* 1960;**35**:313–323.
17. Jacobsen J, Van Deurs B, Pedersen M, Rassing M. TR 146 cells as a model for human buccal epithelium: I Morphology, growth, barrier properties, and permeability. *Int J Pharm* 1995;**125**:165–184.
18. Rupniak HT, Rowlatt C, Lane EB *et al*. Characteristics of four new human cell lines derived from squamous cell carcinomas of the head and neck. *J Natl Cancer Inst* 1985;**75**:621–635.
19. Moharamzadeh K, Brook IM, van Noort R, Scutt AM, Smith KG, Thornhill MH. Development, optimization and characterization of a full-thickness tissue engineered human oral mucosal model for biological assessment of dental biomaterials. *J Mater Sci Mater Med* 2008;**19**:1793–1801.
20. Moharamzadeh K, Franklin KL, Brook IM, van Noort R. Biologic assessment of antiseptic mouthwashes using a three-dimensional human oral mucosal model. *J Periodontol* 2009;**80**:769–775.
21. Vande Vannet BM, Hanssens JL. Cytotoxicity of two bonding adhesives assessed by three-dimensional cell culture. *Angle Orthod* 2007;**77**:716–722.